



Universiteit
Leiden
The Netherlands

The interplay between cholesterol and inflammation in the evolution of atherosclerosis

Verschuren, L.

Citation

Verschuren, L. (2009, January 22). *The interplay between cholesterol and inflammation in the evolution of atherosclerosis*. Retrieved from <https://hdl.handle.net/1887/13415>

Version: Corrected Publisher's Version

License: [Licence agreement concerning inclusion of doctoral thesis in the Institutional Repository of the University of Leiden](#)

Downloaded from: <https://hdl.handle.net/1887/13415>

Note: To cite this publication please use the final published version (if applicable).

Chapter 7

MIF deficiency reduces inflammatory state and impairs development of insulin resistance and associated atherosclerotic disease

Lars Verschuren^{1,2}; Teake Kooistra¹; Jürgen Bernhagen³; Margriet Ouwens⁵; Marjan van Erk⁴; Jitske van der Weij-de Vries¹; Peter Voshol⁶; Ko Willems-van Dijk⁶; Hajo van Bockel²; Günter Fingerle-Rowson⁷; Rick Bucala⁸ and Robert Kleemann^{1,2}

¹ TNO-Quality of Life, Biosciences-Gaubius Laboratory, Leiden, The Netherlands

² Leiden University Medical Center, Dept. of Vascular Surgery, Leiden, The Netherlands

³ RWTH Aachen, Dept. of Biochemistry and Molecular Cell Biology, Aachen, Germany

⁴ TNO-Quality of Life, BioSciences-Bioinformatics, Zeist, The Netherlands

⁵ Radboud University Nijmegen, Nijmegen, The Netherlands.

⁶ Leiden University Medical Center, Dept. of Endocrinology, Leiden, The Netherlands

⁷ Medical Clinic I, Department of Hematology and Oncology, University Hospital Cologne, Cologne, Germany

⁸ Yale University, School of Medicine, Dept. of Medicine and Pathology, New Haven, USA

Submitted

Abstract

Chronic inflammation in white adipose tissue (WAT) is positively associated with obesity, insulin resistance (IR) and the development of type-2 diabetes (T2D). The pro-inflammatory cytokine macrophage migration inhibitory factor (MIF) is an essential, upstream component of the inflammatory cascade. This study examines whether MIF is required for the development of obesity, IR, glucose intolerance and atherosclerosis in the LDL-receptor deficient (Ldlr^{-/-}) mouse model of disease.

Ldlr^{-/-} mice develop IR and glucose intolerance within 15 w while Mif^{-/-}Ldlr^{-/-} littermates are protected. MIF-deficiency does not affect obesity and lipid risk factors but specifically reduces inflammation in WAT and liver, as reflected by lower plasma SAA and fibrinogen levels at baseline and under inflammatory conditions. Conversely, MIF stimulates the *in vivo* expression of human CRP, an inflammation marker and risk factor of IR and cardiovascular disease. In WAT, MIF-deficiency reduces nuclear c-Jun levels and improves insulin sensitivity; MIF-deficiency also reduces macrophage accumulation in WAT and blunts the expression of two proteins that regulate macrophage infiltration (ICAM-1, CD44). Mechanistic parallels to WAT were observed in aorta, where the absence of MIF reduces monocyte adhesion, macrophage lesion content and atherosclerotic lesion size.

These data highlight the physiological importance of chronic inflammation in development of IR and atherosclerosis, and suggest that MIF is a potential therapeutic target for reducing the inflammatory component of metabolic and cardiovascular disorders.

Introduction

The intertwined medical problems of obesity, glucose intolerance, type-2 diabetes (T2D), dyslipidemia and atherosclerosis form one of the most serious threats to public health, worldwide. Insulin resistance (IR) is as an integral feature of the medical sequelae that are collectively referred to as the metabolic syndrome¹. Decreased insulin sensitivity is the underlying defect in >90% of patients with T2D, and it is also considered to be a major pathologic mechanism for the associated development of cardiovascular disease (CVD)². Recent human population and experimental animal studies have established both correlative and causative links between IR and chronic inflammation, in particular within adipose tissue^{3;4}. For example, C-reactive protein (CRP), which is a serum marker of systemic inflammation, is independently related to insulin insensitivity (Insulin Resistance Atherosclerosis Study; 1,008 non-diabetic subjects⁵) and highly predictive for progression to overt T2D⁶. Mechanistic studies that have evaluated the impact of blocking specific inflammatory control points, such as c-Jun N-terminal kinase 1 (JNK1) transcription factor⁷, support the concept that the persistent activation of pro-inflammatory transcription factors (e.g. c-Jun) in critical metabolic sites (adipose and liver tissue) may underlie the development of IR. When chronically inflamed, these tissues release pro-inflammatory molecules, including cytokines, acute-phase reactants and pro-coagulant factors (e.g. IL-6, SAA, CRP, fibrinogen), which can participate in the pathogenesis of IR and atherosclerosis^{3;8-10}. A primary event in the pathogenesis of IR is the infiltration of macrophages into white adipose tissue (WAT). This process appears to be of critical importance for the development of low-grade adipose tissue inflammation, and it may be a unifying mechanism for the development of IR and atherosclerosis³. Nevertheless, our understanding of the factors that contribute to WAT inflammation is incomplete, and from a therapeutic perspective it remains unclear if inflammatory pathways can be therapeutically manipulated for clinical benefit.

Macrophage migration inhibitory factor (MIF) is a widely expressed pro-inflammatory cytokine that participates in the development of many inflammatory disorders, including those that contribute to cardiovascular disease¹¹⁻¹⁴. MIF amplifies the pro-inflammatory cascade and it controls the 'set point' and the magnitude of inflammatory responses, including those mediated by JNK1^{11;15}. In a recent study, we showed that MIF can exert chemokine-like functions and enhance the tissue infiltration of macrophages during atherogenesis¹⁶.

Here, we have investigated whether genetic deletion of *mif* would result in a lower systemic and/or lower WAT-specific inflammation, and whether reducing MIF-dependent inflammation would prevent the evolution of IR, glucose intolerance and associated CVD. The LDL receptor-deficient mouse (Ldlr^{-/-}) was chosen as a model because IR and atherosclerosis develop sequentially¹⁷ and under the mild conditions of a chow diet thereby mimicking the slow progression of disease in humans. Disease evolution and inflammation was monitored using established metabolic and inflammation markers. Parallel glucose tolerance testing and hyperinsulinemic-euglycemic clamp analysis in combination with functional, genome-wide pathway analysis and immunohistochemistry enabled us to explore for the first time the role of MIF in a chronic setting of acquired IR and atherosclerosis.

Methods

Animals and diets

All lines used had a C57BL/6 background. Atherosclerosis-prone Ldlr^{-/-} mice were crossbred with Mif^{-/-} mice to establish an Ldlr^{-/-}Mif^{-/-} double transgenic line. Male littermates derived from crossbreeding of Ldlr^{-/-}Mif^{+/-} mice were used for the metabolic cage experiments, glucose tolerance tests, insulin tolerance tests, the hyperinsulinemic euglycemic clamp analysis, and the atherosclerosis experiments. Mice were genotyped by PCR and Western blotting confirming absence of Mif and Ldlr expression in the respective knock-outs. Human CRP (huCRP) transgenic mice were characterized by PCR and ELISA for huCRP expression and challenged with cytokines essentially as described.¹⁸ Animal experiments were approved by the Institutional Animal Care and Use Committee of The Netherlands Organization for Applied Scientific Research (TNO) and were in compliance with European Community specifications regarding the use of laboratory animals.

Analyses of plasma lipids and proteins

Total plasma cholesterol and triglyceride levels were measured after 4 hours of fasting, using kits No. 11489437 and 11488872 (Roche Diagnostics, Almere, The Netherlands), respectively.¹⁹ For lipoprotein profiles, pooled plasma was fractionated using an ÅKTA FPLC system (Pharmacia, Roosendaal, The Netherlands).²⁰ The plasma levels of serum amyloid A (SAA) were determined by ELISA (Biosource) as reported.⁸ Fibrinogen was determined with an in-house ELISA.¹⁹ Adiponectin, leptin, E-selectin, and VCAM-1 were quantified by established ELISA (R&D Systems Europe, Ltd., Abingdon, United Kingdom).

Analyses in computerized metabolic cages

Animals received a standard chow diet and were acclimatized to the metabolic cage environment for 1 day prior to starting of the monitoring period. During the metabolic cage experiment, O₂ consumption, CO₂ production, food and water intake, and activity (x-y-z-axis) were monitored.²¹ After a 50 h period, chow diets were removed and animals received a diabetogenic high fat diet containing 24% w/w beef tallow for another 50 h. Respiratory exchange ratio (RER) and energy expenditure were calculated from the data collected.

Glucose and insulin tolerance tests.

After a 4-h fast, mice were injected intraperitoneally with glucose (2 g/kg body weight). Blood samples were taken at various time points (0–120 min), and blood glucose was determined with hand-held glucose analyzer (FreeStyle; Disetronics, Vianen, The Netherlands). For insulin tolerance tests, 4-h fasted mice were treated intraperitoneally with human insulin (0.5 U /25 g body weight). Blood samples were taken at various time points (0–90 min) and blood glucose was measured as described above.

Hyperinsulinemic euglycemic clamp analysis

The clamp experiments were performed as described.²² Briefly, after an overnight fast, animals were anesthetized (0.5 mL/kg Hypnorm; Janssen Pharmaceutica, Berchem, Belgium and 12.5 mg/g midazolam; Genthon BV, Nijmegen, The Netherlands) and an infusion needle was placed in one of the tail veins. Subsequently, a bolus of insulin (200 mU/kg; Actrapid, Novo Nordisk, Chartres, France) was given, and a hyperinsulinemic euglycemic clamp was started with a continuous infusion of insulin (7.0 mU/min · kg) and a variable infusion of 12.5% D-glucose (in phosphate-buffered saline [PBS]) to maintain blood glucose level at about 7.5 mmol/L. Blood samples were taken every 5 to 10 minutes and plasma glucose levels were monitored using a hand-glucose meter (FreeStyle; Disetronics, Vianen, The Netherlands). Glucose infusion rate was calculated as described.²²

Western Blotting and co-immunoprecipitation

Tissue extracts were prepared in the presence of proteinase inhibitors (PI) (Roche Diagnostics) and Western blotting experiments were performed following detailed protocols using anti-MIF antibodies (sc-2012; sc-16965) and an anti- β -actin (sc-1615) control antibody. All primary and secondary antibodies were obtained from Santa Cruz Biotechnology (Heerhugowaard, The Netherlands). Immunoblots were visualized using the Super Signal West Dura Extended Duration Substrate (Pierce, St Augustin, Germany) and the luminescent image workstation (Roche Diagnostics).

Assay of PI 3-kinase activity

PI-3-kinase activity was quantified as reported.²³ Briefly, 50 μ l of a reaction mixture containing 0.2 mg/ml PI, 20 mM HEPES, pH 7.2, 0.4 mM EGTA, 0.4 mM Na₂HPO₄, and 10 mM MgCl₂ with or without wortmannin (1 μ M) were added to the immunoprecipitates. The kinase buffer was incubated with the immunoprecipitates for 5 min at room temperature, and the reaction was started by addition of [³²P]ATP (40 μ M and 0.2 μ Ci/ μ l). After 20 min, the reaction was stopped by the addition of 30 μ l of 4 N HCl and 130 μ l of chloroform-methanol (1/1). The organic phase was extracted and spotted on a silica gel thin-layer chromatography plate (Merck, Darmstadt, Germany) and was developed in chloroform-methanol-25% NH₄OH-water (43:38:5:7, v/v). Plates were dried and subsequently visualized.

Nucleic acid extraction and microarray analysis

Total RNA was extracted from epididymal adipose tissue (n=5 per group) using RNAzol (Campro Scientific, Veenendaal, The Netherlands) and glass beads according to the manufacturer's instructions. Integrity of RNA obtained was examined by Agilent Lab-on-a-chip technology using the RNA 6000 Nano LabChip kit and a bioanalyzer 2100 (Agilent Technologies, Amstelveen, The Netherlands) essentially as described

recently.⁸ The One-Cycle Target Labeling and Control Reagent kit (Affymetrix #900493) and the protocols established by Affymetrix were used to prepare biotinylated cRNA (from 5 µg of total RNA) for microarray hybridization. The quality of intermediate products (i.e. biotin-labeled cRNA and fragmented cRNA) was again controlled using the RNA 6000 Nano Lab-on-a-chip and bioanalyzer 2100. Microarray analysis was carried out using an Affymetrix technology platform and Affymetrix GeneChip® mouse full genome 430 2.0 arrays (45,037 probe sets; 34,000 well-characterized mouse genes). Briefly, fragmented cRNA was mixed with spiked controls, applied to Affymetrix Test chips, and good quality samples were then used to hybridize with murine GeneChip® 430 2.0 arrays.⁸ The hybridization, probe array washing and staining, and washing procedures were executed as described in the Affymetrix protocols, and probe arrays were scanned with a Hewlett-Packard Gene Array Scanner (Leiden Genome Technology Center, Leiden, The Netherlands).

For parallel quantitative real-time polymerase chain reaction (qRT-PCR) analysis, an published procedure²⁴ was followed: a mastermix (Eurogentec, Seraing, Belgium), an ABI-7700 system (PE Biosystems, Nieuwekerk a/d IJssel, The Netherlands) and established primer/probe sets were used according to the manufacturer's instructions with cyclophilin (PE Biosystems) as a reference.

Gene expression data analysis

Microarray data analysis was carried out essentially as described in detail in a recent study.⁸ Briefly, raw signal intensities were normalized using the GCRMA algorithm (Affy package in R). Datasets are freely accessible online through ArrayExpress (<http://www.ebi.ac.uk/arrayexpress>). Statistical analysis was performed in BRB ArrayTools (Dr. Richard Simon and Amy Peng Lam, <http://linus.nci.nih.gov/BRB-ArrayTools.html>). Gene expression datasets of Ldlr^{-/-} and Mif^{-/-} Ldlr^{-/-} were tested for differentially expressed genes using class comparisons with multiple testing corrections by estimation of false discovery rate (FDR). Differentially expressed genes were identified at a threshold for significance of $\alpha < 0.01$ and a FDR < 5%. Within the set of differentially expressed genes, a Student's *t*-test was carried out to analyze differential expression of individual genes between the Ldlr^{-/-} group and the Mif^{-/-} Ldlr^{-/-} group.

For biological interpretation of the differentially expressed genes, MetaCore™ (GeneGo Inc., USA) was used. Enrichment of Biological Processes (Gene Ontology annotation) was analyzed in MetaCore™.⁸

Immunohistochemical analysis of adipose tissue

Direct after sacrifice, adipose tissues were fixed in formalin and embedded in paraffin to prepare cross sections (5 µm thick) for immunohistological analysis. For immunostaining of macrophages, c-Jun, CD44 and ICAM, we used antibodies MAC-3 (BD Biosciences Pharmingen), sc-45, sc-18849 (both Santa Cruz Biotechnology) and GTX76543 (Genetex), respectively. Biotin (Jackson ImmunoResearch) and Alexa Fluor488 (Invitrogen) labelled secondary antibodies were used for immunofluorescence according to an established staining protocol.¹⁹ Stained cross sections were covered in malinol or Vectashield with DAPI (Vector Laboratories) as mounting medium. Olympus BX51 microscope and CELL^D software (Olympus, Zoeterwoude, The Netherlands) were used for morphometric computer-assisted analysis. A custom-made analysis-module within the CELL^D software was created for the analysis of adipocyte size. Partially captured adipocytes were not analyzed. A comparable area was analyzed for Ldlr^{-/-} and Mif^{-/-} Ldlr^{-/-}.

Analyses of atherosclerosis

Total aortic plaque load was determined in longitudinally opened Oil red O-stained aortas following an established procedure.¹⁹ To analyze atherosclerosis in the aortic valve area (aortic root) hearts were fixed and embedded in paraffin. Serial cross sections (5 μm thick) were prepared throughout the entire aortic valve area and stained with hematoxylin-phloxine-saffron (HPS). Atherosclerosis was analyzed blindly in four cross-sections of each specimen (at intervals of 30 μm) as reported.¹⁹ QWin-software (Leica) was used for morphometric computer-assisted analysis of lesion area as described in detail elsewhere.¹⁹ Monocytes and macrophages were immunostained in cross sections adjacent to the ones used for quantification of atherosclerosis using AIA31240 (1:3000, Accurate Chemical and Scientific, Brussels, Belgium) to determine the number of monocytes attached to the endothelium, the macrophage-containing lesion area. Significance of differences was calculated by one-way analysis of variance (ANOVA) test followed by a least significant difference (LSD) post hoc analysis using SPSS 11.5 for Windows (SPSS, Chicago, USA). The level of statistical significance was set at $P < 0.05$.

Results

Effect of MIF-deficiency on lipids and metabolic markers

Ldlr^{-/-} mice and Mif^{-/-}Ldlr^{-/-} littermates were fed a chow diet for 35 weeks and risk factors of the metabolic syndrome were monitored over time. The plasma levels of cholesterol, triglycerides and free fatty acids were comparable in both groups of mice (Table 1 shows values at $t=12$ and $t=35$ weeks). Ldlr^{-/-} and Mif^{-/-}Ldlr^{-/-} mice also had similar lipoprotein profiles indicating that the presence or absence of MIF does not affect the level of VLDL, LDL and HDL (Figure 1A).

Fasting plasma insulin concentrations at 12 weeks of age tended to be lower in Mif^{-/-}Ldlr^{-/-} (0.77 ± 0.09 mM versus 1.27 ± 0.38 mM), and this difference became significant at week 35 because insulin levels increased strongly in Ldlr^{-/-} (4.0 ± 0.7 mM) but only moderately in Mif^{-/-}Ldlr^{-/-} mice (1.9 ± 0.2 mM; Figure 1B). A similar picture was also obtained for glucose: While fasting blood glucose levels were comparable at 12 weeks of age (8.0 ± 1.6 mM in Ldlr^{-/-} and 7.6 ± 1.4 mM Mif^{-/-}Ldlr^{-/-} mice), with increasing age a significant difference emerged at week 35 because glucose levels increased in Ldlr^{-/-} mice (10.2 ± 2.0 mM) while remaining low in Mif^{-/-}Ldlr^{-/-} mice (7.3 ± 1.0 mM) (Figure 1C).

Calculation of the HOMA index as a measure of IR in week 12 and 35 revealed a strong increase in Ldlr^{-/-} mice (from 0.3 ± 0.1 to 1.9 ± 0.4). In contrast, HOMA hardly increased in Mif^{-/-}Ldlr^{-/-} (from 0.2 ± 0.05 to 0.6 ± 0.02) (Figure 1D). These data show that Mif^{-/-}Ldlr^{-/-} mice are protected from developing hyperinsulinemia and hyperglycemia, which suggests that MIF has a role in the development of IR.

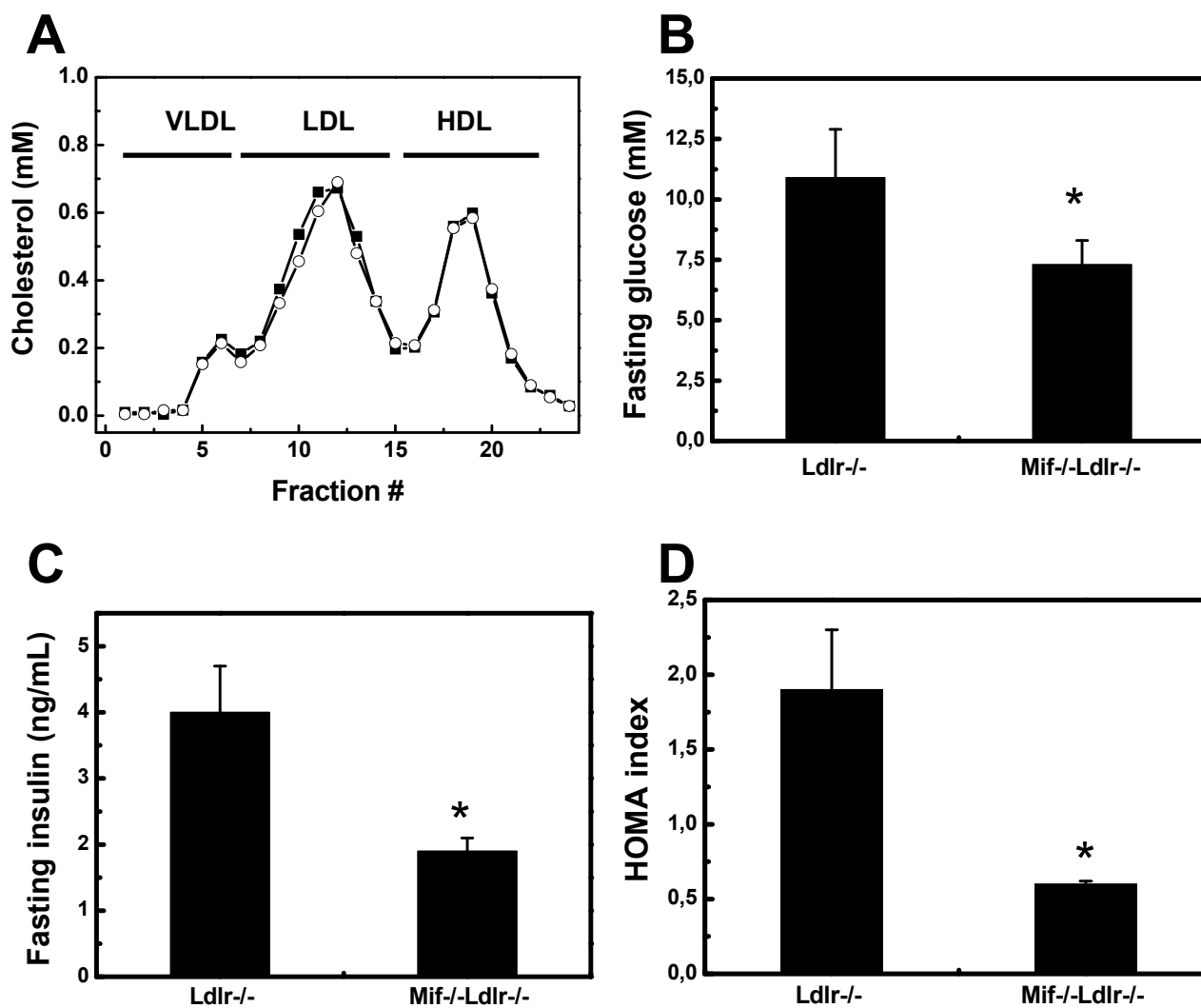


Figure 1: **A**, Lipoprotein profiles of the Ldlr^{-/-} (open circles) and Mif^{-/-}Ldlr^{-/-} (solid squares) mice on a maintenance (chow) diet assessed by FPLC-based size-exclusion method (ÅKTA) and subsequent determination of cholesterol in the collected fractions. **B**, Average fasting whole blood glucose levels, **C**, average fasting plasma insulin levels and **D**, HOMA values of Ldlr^{-/-} and Mif^{-/-}Ldlr^{-/-} mice. Significant difference is indicated * P<0.05.

There was no difference in food intake between the groups during the treatment and Mif^{-/-}Ldlr^{-/-} mice had a slightly lower body weight (not significant) (Table 1). Also when the treatment was prolonged (up to 52 weeks), there was no significant effect on body weight: both groups became obese and the average body weight was 46.9±5.6 g in Ldlr^{-/-} and 44.1±7.2 g in Mif^{-/-}Ldlr^{-/-}. The mass of subcutaneous, visceral and epididymal fat was also comparable in Ldlr^{-/-} and Mif^{-/-}Ldlr^{-/-} mice (sc: 1.45±0.37 g vs. 1.79±0.61 g; visc: 0.71±0.12 g vs. 0.66±0.30 g; epi: 1.38±0.47 g vs. 1.26±0.43 g in week 52) and plasma leptin levels were similar in the two strains (Table 1).

	12 w old		35 w old	
	Ldlr-/-	Mif-/- Ldlr-/-	Ldlr-/-	Mif-/- Ldlr-/-
Food intake [g/day]	5.4 ± 0.5	5.0 ± 0.7	4.6 ± 0.3	4.9 ± 0.3
Body weight (start) [g]	28.4 ± 2.9	28.6 ± 2.9	38.2±5.4	36.1±4.6 g
Plasma adiponectin [mg/mL]	ND	ND	8.0±1.7	8.3±2.6
Plasma leptin [ng/ml]	3.5 ± 1.9	3.4 ± 2.5	146.1±47.3	146.3±54.8
Plasma cholesterol [mM]	5.6 ± 1.0	5.7 ± 1.3	11.4±1.7	14.0± 3.3
Plasma triglyceride [mM]	1.7 ± 0.4	1.6 ± 0.3	2.6±0.7	2.9±1.3
Plasma free fatty acid [mM]	0.84 ± 0.19	0.87 ± 0.23	0.50± 0.20	0.61± 0.13
Plasma fibrinogen [mg/mL]	2.4 ± 0.8	1.8 ± 0.5	4.7 ± 0.8	3.0 ± 0.4*
Plasma SAA [µg/ml]	8.4 ± 4.9	2.4 ± 1.0*	109 ± 14	10 ± 7*

Table 1: Effects of MIF-deficiency on markers of cardiovascular and metabolic disease. Data are presented as mean ± SD. *P<0.05 between groups.

MIF-deficiency lowers chronic inflammation and reduces the magnitude of the inflammatory response

Serum amyloid A (SAA) is a circulating inflammation marker produced by liver and adipose tissue. SAA levels were significantly lower in Mif-/-Ldlr-/- mice already at week 12 (Table 1), i.e. at a time point at which Ldlr-/- and Mif-/-Ldlr-/- still had comparable levels of insulin and glucose. While SAA levels strongly increased in Ldlr-/- (up to 109±14 µg/mL at 35 weeks), they remained low in Mif-/-Ldlr-/- (10±7 µg/mL). Mif-/-Ldlr-/- also displayed significantly lower levels of fibrinogen, a liver-specific marker of inflammation (Table 1). Our finding that MIF influences the inflammatory status was also confirmed in normolipidemic C57BL/6 mice. Plasma SAA and fibrinogen concentrations were 70±11 µg/mL and 3.3±1.1 mg/mL in MIF-expressing C57BL/6 whereas MIF-deficient littermates displayed significantly lower levels (7±1 µg/mL and 2.7±0.8 mg/mL, P<0.05; not shown). In an independent experiment, the metabolic performance of Ldlr-/- and Mif-/-Ldlr-/- mice was analyzed in more detail. Mice were housed individually in computerized metabolic cages with free access to water and chow. There was no significant difference in voluntary activity, food intake, water consumption, O₂ consumption and CO₂ production. (Supplementary information in appendix I, page 157). In both groups, the respiratory

exchange rate (RER) varied between 0.9 (night) and 1 (day) indicating that mice predominantly used glucose in chow as an energy substrate.

Stimulation experiments with a prototypic trigger of inflammation, IL-1 β , revealed that MIF also determined the magnitude of an inflammatory response. Ldlr $^{-/-}$ and Mif $^{-/-}$ -Ldlr $^{-/-}$ were intraperitoneally challenged with IL-1 β (125000 U/25 g body weight). Plasma SAA was quantified 18 h after IL-1 β injection, which is a time point for which stimulation previously had been determined to be maximal (not shown). IL-1 β stimulation resulted in an inflammatory response and significantly increased plasma SAA levels in Ldlr $^{-/-}$ mice (Figure 2A). In Mif $^{-/-}$ -Ldlr $^{-/-}$ mice however, plasma SAA remained low, even at a later time point (not shown). Reconstitution of Mif $^{-/-}$ -Ldlr $^{-/-}$ mice with recombinant MIF (single i.p. injection of 10 μ g of LPS-free rMIF 15 h prior to IL-1 β induction) resulted in baseline and IL-1-stimulated SAA levels that were comparable to those observed in Ldlr $^{-/-}$ mice (Figure 2A).

The expression of human CRP, which is a sensitive marker of chronic inflammation and a predictor of metabolic and cardiovascular disease, was induced by recombinant MIF (rMIF) as shown in Figure 2B: Mice transgenic for human CRP (CRPtg) responded to rMIF (10 μ g; i.p.) with a significant increase (2.6-fold) in plasma CRP concentrations. The effect of MIF on CRP was time- and dose-dependent, and maximal 18 h after stimulation (not shown). MIF was less potent than IL-1 β (9-fold increase of CRP, not shown), which is a well-established stimulator of CRP in this model. Protein mutants of MIF, i.e. C60S-MIF or P2A-MIF, which lack the intrinsic catalytic activity of MIF and have been found to also lack inflammatory activities^{25,26} did not stimulate CRP expression in CRPtg mice, thereby confirming that the effect of MIF on CRP was specific (Figure 2B). Consistent with this notion, rMIF but not the mutant proteins stimulated human CRP promoter activity in human HuH7 hepatoma cells transiently transfected with a plasmid containing a 300 bp fragment of the human CRP promoter cloned in front of a luciferase reporter gene. The CRP promoter-activating effect of MIF alone was about 2-fold (not shown) and additive to the stimulating effect of IL-1 (Supplementary Information, appendix II, page 158). Also, MIF stimulated the basal and IL-1-induced activity of the promoter of IL-6, the principle cytokine inducer of CRP (Supplementary Information, appendix II, page 158).

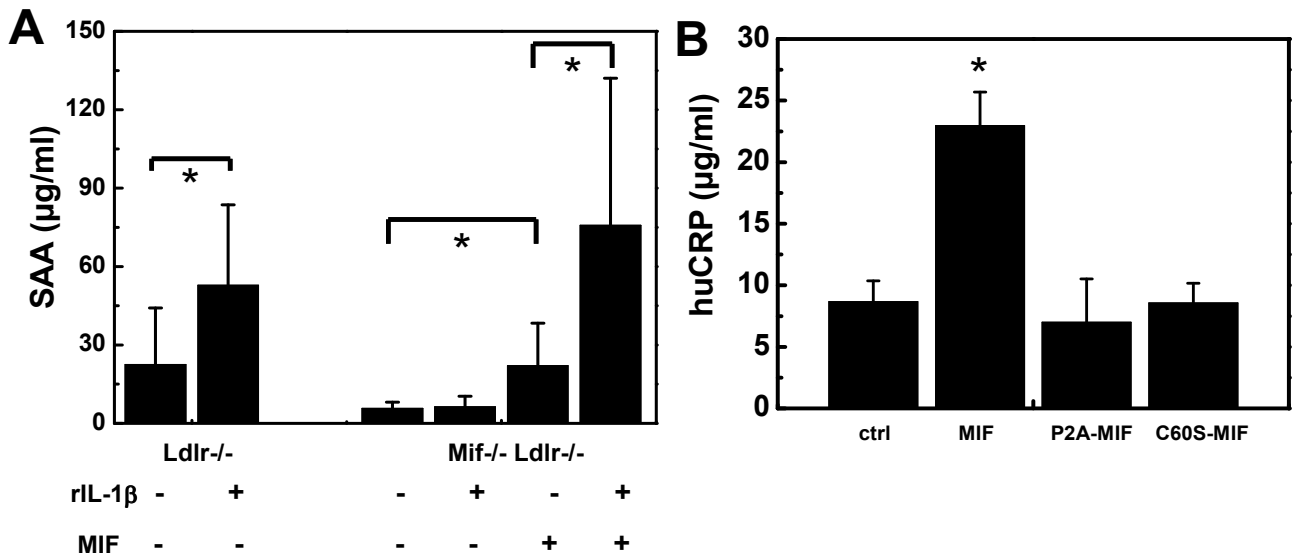


Figure 2: **A**, Plasma SAA levels 18 h after stimulation of Ldlr^{-/-} and Mif^{-/-}Ldlr^{-/-} mice with recombinant IL-1 β . In Mif^{-/-}Ldlr^{-/-} mice, MIF was reconstituted by i.p. administration of recombinant human MIF protein (MIF; 10 μg ; free of LPS (<1pg endotoxin/ μg MIF protein) as assessed by Limulus Amoebocyte Lysate assay). **B**, Human CRP levels in human CRP transgenic mice 18 h after stimulation with either MIF or P2A-MIF lacking tautomerase activity or C60S-MIF lacking oxidoreductase activity (all 10 μg ; i.p.). Data shown are absolute values and expressed as means \pm S.D. Significant difference is indicated * P <0.05.

MIF-deficiency protects against the development of glucose intolerance and IR

To examine whether a reduction in chronic, low-grade inflammation by deleting *mif* would affect the development of IR, we subjected Ldlr^{-/-} and Mif^{-/-}Ldlr^{-/-} mice (12 weeks of age) to glucose tolerance and insulin tolerance tests. In the presence of MIF, peak glucose levels normalized later and Ldlr^{-/-} mice had a significantly higher AUC than Ldlr^{-/-}Mif^{-/-} (AUC: 817 \pm 353 vs. 507 \pm 174; P <0.05 Figure 3A). The difference in glucose tolerance became even more pronounced at later time points. At 35 weeks, the AUC was 1225 \pm 397 in Ldlr^{-/-} but stayed at 519 \pm 194 in Ldlr^{-/-}Mif^{-/-}; P <0.001 (Figure 3B). Insulin levels did not differ significantly during glucose tolerance testing (not shown).

Subsequent insulin tolerance tests revealed that the clearance of plasma glucose occurred more efficiently (i.e. more rapidly within the first 15 min; P <0.05) in Ldlr^{-/-}Mif^{-/-} mice, (Figure 3C), which suggests that a difference in insulin sensitivity may exist. In line with this notion, hyperinsulinemic-euglycemic clamp analysis showed that the glucose infusion rate in Ldlr^{-/-}Mif^{-/-} mice was greater than in Ldlr^{-/-} (14.0 \pm 3.4 vs 8.6 \pm 3.7 mg/kg.min; P <0.05) indicating that the presence of MIF may promote the development of IR (Figure 3D).

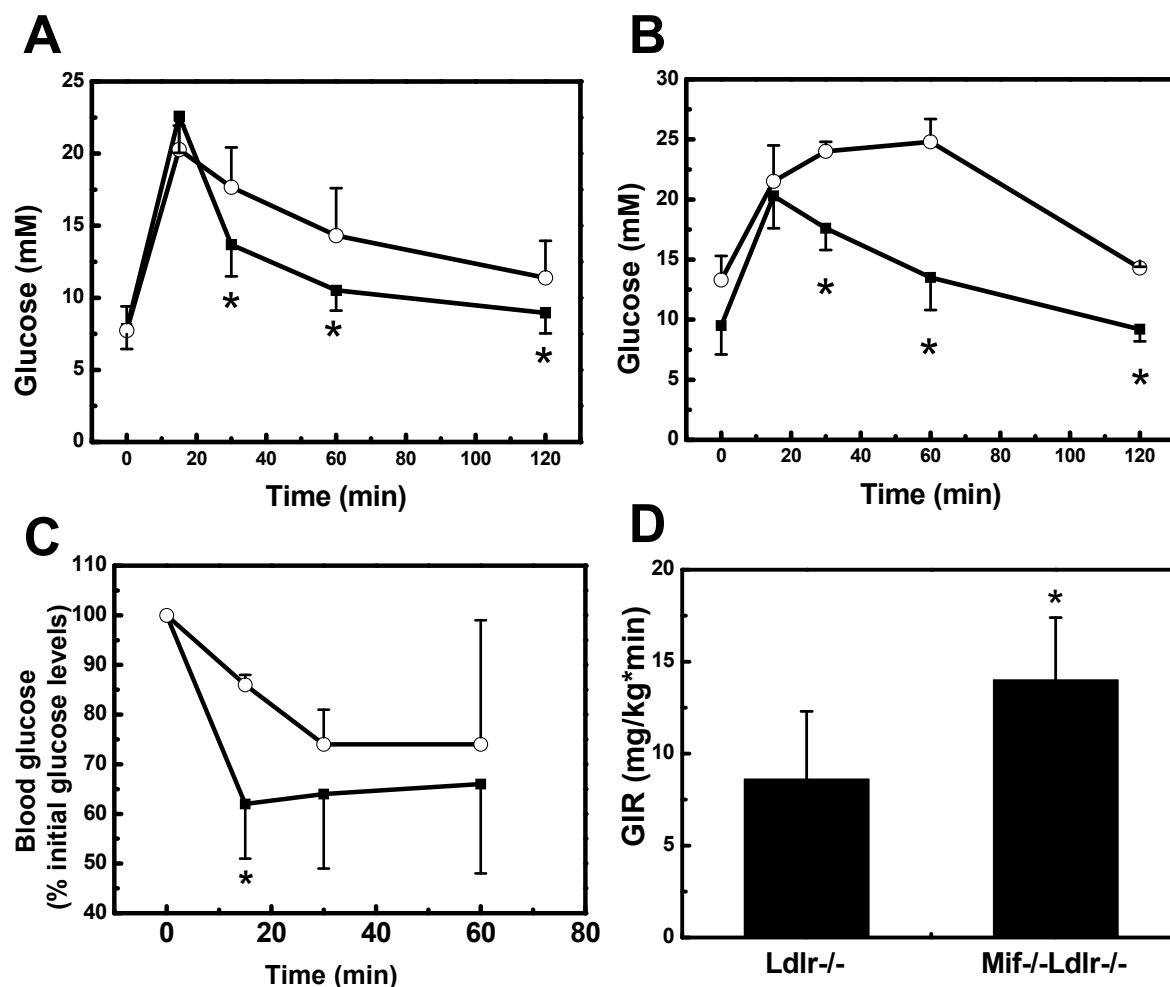


Figure 3: **A**, Glucose tolerance test in Ldlr-/- (open circles) and Mif-/-Ldlr-/- (solid squares) mice at 12 weeks of age and **B**, at 35 weeks of age. **C**, Insulin tolerance test in Ldlr-/- (open circles) and Mif-/-Ldlr-/- (solid squares) mice. **C**, Determination of whole body insulin resistance by euglycemic hyperinsulinemic clamp analysis. Data shown are absolute values and expressed as means \pm S.D. Significant difference between the groups is indicated * $P < 0.05$.

MIF-deficiency reduces the inflammatory state of WAT

Because the circulating levels of inflammatory markers were lower in Mif-/-Ldlr-/- mice, we analyzed the inflammatory status of liver and WAT. Western blot analysis of tissue homogenates showed that MIF is expressed in liver and WAT of Ldlr-/- mice (Figure 4A). A parallel IHC analysis demonstrated MIF immunoreactivity in all cell types present in these tissues (not shown).

The liver tissue of Ldlr-/- mice showed slight c-Jun immunoreactivity but there was no significant difference in either c-Jun or p-c-Jun immunoreactivity when these mice were compared to Mif-/-Ldlr-/- littermates (not shown). The expression of hepatic genes encoding enzymes that control glucose homeostasis/*de novo* synthesis (phosphoenolpyruvate carboxykinase, glucose-6-phosphatase) also was comparable in both groups (not shown).

Histological analysis of WAT revealed smaller adipocytes in Mif^{-/-}Ldlr^{-/-} mice when compared to Ldlr^{-/-}, and computerized quantification of adipocyte size demonstrated a significant difference. The peak size of adipocytes in Ldlr^{-/-} was 1500 to 1800 μm^2 , whereas in Mif^{-/-}Ldlr^{-/-} mice it was only 600 to 900 μm^2 (Figure 4B).

Specific staining of macrophages (anti-MAC3) showed that the WAT of Mif^{-/-}Ldlr^{-/-} contained significantly fewer macrophages and fewer crown-like structures (Figure 4C and Supplementary Information, appendix III, page 159). In Ldlr^{-/-} mice, pronounced c-Jun immunoreactivity (Figure 4D) was observed in MAC3-positive areas as well as in adipocytes. Merging the immunofluorescent signals of c-Jun and nuclear DAPI revealed that a substantial amount of c-Jun was associated to the nucleus (Figure 4E-G). Nuclear c-Jun immunoreactivity was predominantly found in adipocytes that were in close proximity to macrophages/crown-like structures but such staining was less evident in more distant adipocytes. In WAT from Ldlr^{-/-}Mif^{-/-} mice, c-Jun immunoreactivity was less intense and mainly cytosolic.

A comparison of WAT from Mif^{-/-}Ldlr^{-/-} and Ldlr^{-/-} by functional microarray analysis across pathways showed that the major changes in gene expression occur in the functional categories 'cell signaling', 'cell cycle control', 'immune response' and 'lipid metabolism'. Within the category 'cell signaling', the insulin-sensitive processes 'leptin signaling via JAK/STAT and MAPK cascades' and 'IGF-R1 signaling' were differentially affected (Supplementary Information, appendix IV, page 160). These data, considered together with the IHC analysis of c-Jun, suggest an effect of MIF on insulin sensitivity.

As a direct test of the influence of MIF on the insulin signaling cascade, we injected insulin (i.p.; 0.5 U insulin/25 g body weight) into Ldlr^{-/-} and Mif^{-/-}Ldlr^{-/-} littermates. Mice were sacrificed 10 min after injection (insulin dose and time point of sacrifice had been optimized in previous scouting experiments) and the IRS1-associated PI3-kinase activity was determined as a functional measure of the insulin signaling route. PI3-kinase activity was significantly higher in WAT of Mif^{-/-}Ldlr^{-/-} mice when compared to Ldlr^{-/-} mice (Figure 5A).

The biological relevance of this effect was supported further by the higher levels of phospho-AKT, a downstream effector of PI3-kinase, in WAT of Mif^{-/-}Ldlr^{-/-} mice (Figure 5B). No difference in PI3-kinase activity and phospho-AKT levels in liver and muscle were observed (Supplementary Information, appendix V, page 161).

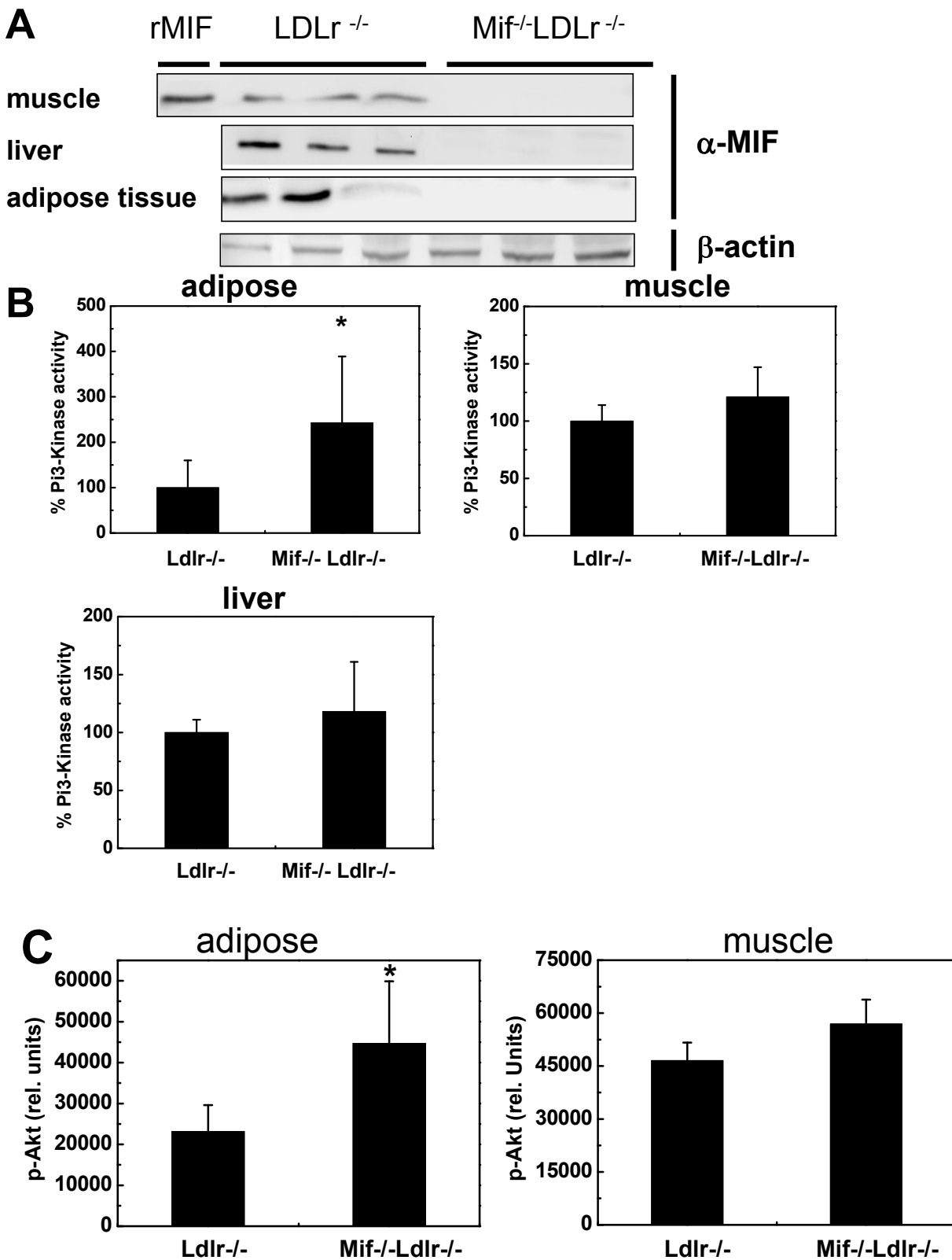


Figure 4: A, Western blot analysis of Mif in tissue homogenates of Ldlr^{-/-} and Mif^{-/-}Ldlr^{-/-} mice. B, PI3-kinase activity in Ldlr^{-/-} and Ldlr^{-/-}Mif^{-/-} mice. C, p-AKT levels in peripheral tissues of Ldlr^{-/-} and Ldlr^{-/-}Mif^{-/-} mice as assessed by Western blotting. Data shown are expressed as means \pm S.D. *indicates a significant difference between the groups ($P < 0.05$).

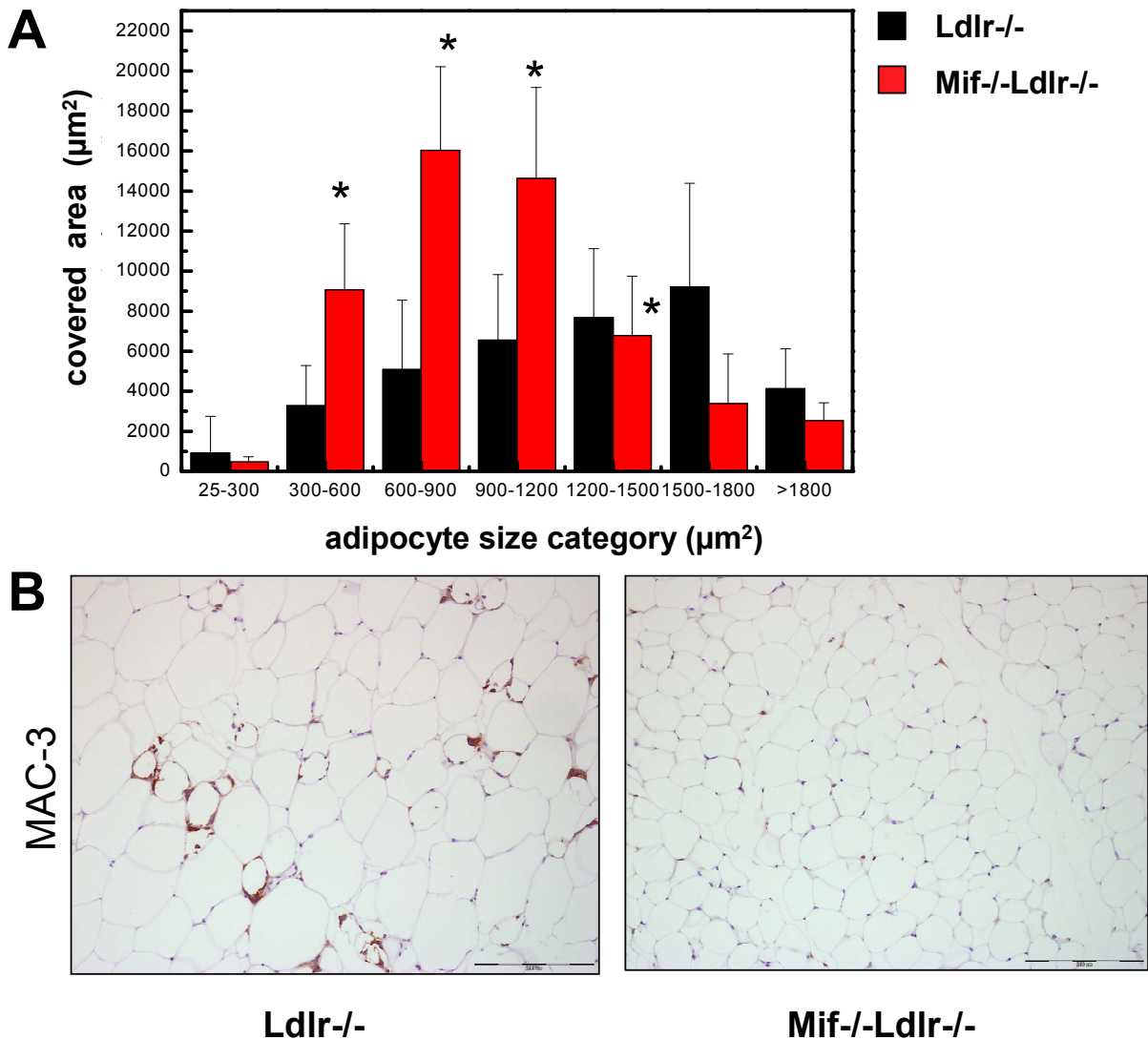


Figure 5: A, Computer-assisted quantification of adipocyte size in Ldlr^{-/-} (black bars) and Mif^{-/-}Ldlr^{-/-} (red bars) mice. Adipocytes were classified into groups on basis of their size (µm²; size categories on x-axis). The figure depicts the area that is covered by adipocytes of a specific size. Data shown are absolute values and expressed as means ± S.D. Significant difference is indicated * P<0.05. **B**, Representative photomicrographs of epididymal adipose tissue from Ldlr^{-/-} and Mif^{-/-}Ldlr^{-/-} mice stained with a macrophage-specific antibody (MAC-3). (Figure 5 is continued on next page)

MIF-deficiency blocks macrophage infiltration into WAT

Pathway analysis of the WAT transcriptome dataset showed that the presence of MIF was significantly associated with the inflammatory processes 'IL-1 and IL-6 signaling', 'ERK activation', 'IL-3 activation and signaling' and 'cell adhesion' (all P<0.05; not shown). Consistent with the enhanced inflammatory status of MIF-expressing, Ldlr^{-/-} mice the genes encoding for chemokines (Ccl2, Ccl9, Ccr5, Ccl6), proteases (Mmp12), complement components (C1qb, C1qa, C3ar3, C3ar1), acute phase proteins (Mup-1, Orm2, SAA3), cell

adhesion/immune cell recruitment factors (Cd9, Cd44, Cd84, Cd72) also were significantly

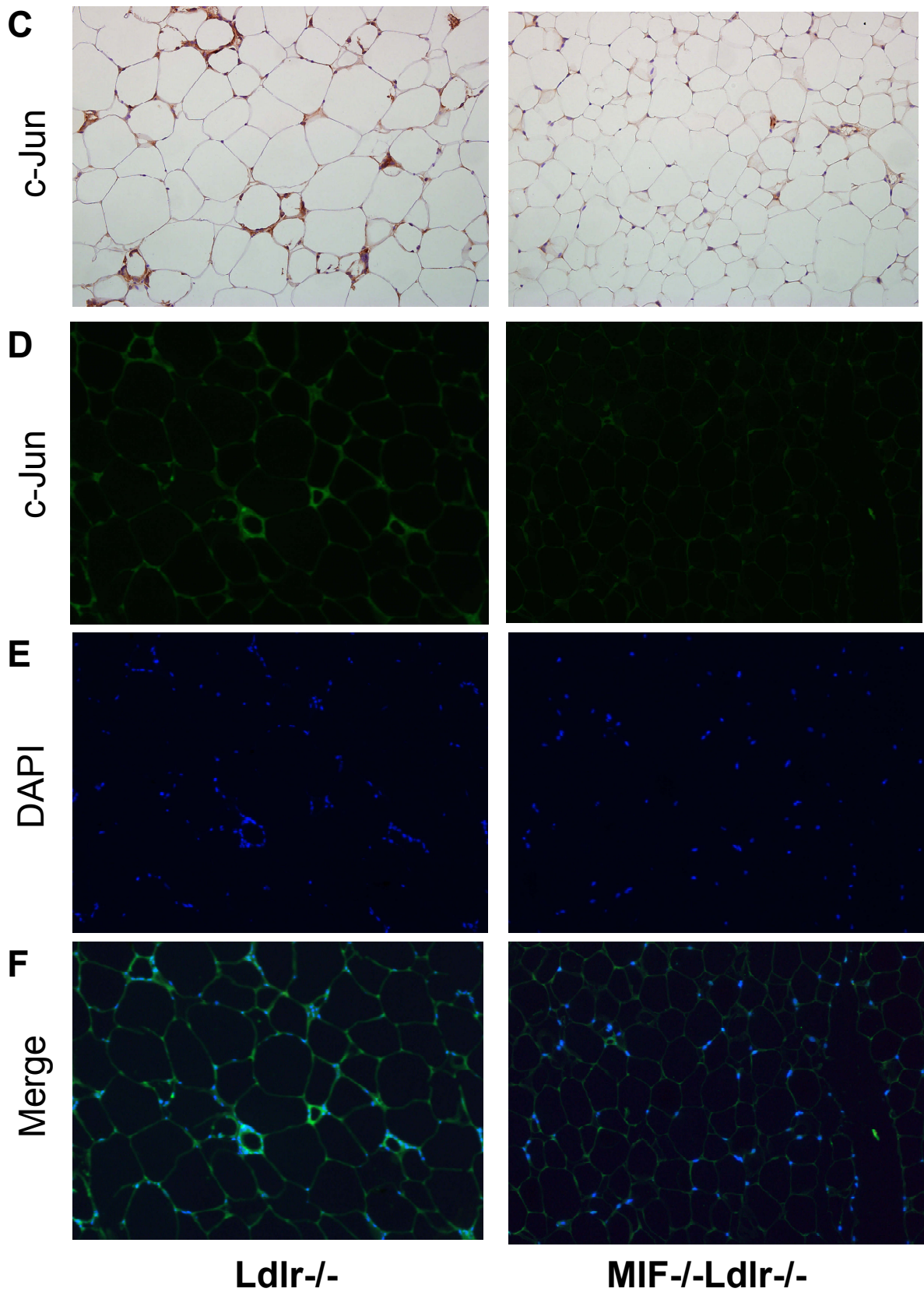


Figure 5: (continued) **C**, a c-Jun specific antibody detected with Nova Red or **D**, a c-Jun specific antibody detected with fluorescent labelled secondary antibody or **E**, with DAPI for staining of nuclei; **F**, Merged photomicrographs showing that c-Jun-IR is nuclear.

($P < 0.01$) upregulated, suggesting that MIF promotes the recruitment of immune cells into adipose tissue. To better substantiate this observation, we measured the expression level of proteins that mediate monocyte/macrophage recruitment into WAT. Circulating levels of VCAM-1 and ICAM-1 were significantly lower in *Mif*^{-/-}*Ldlr*^{-/-} mice compared to *Ldlr*^{-/-} (Figure 6A,B). IHC staining of the cell adhesion molecules ICAM and CD44 in cross-sections of WAT showed pronounced ICAM- and CD44 levels in *Ldlr*^{-/-} mice. CD44 was predominantly detected in MAC3-positive cells of crown-like structures. ICAM-1 and CD44 staining was markedly and significantly reduced in *Mif*^{-/-}*Ldlr*^{-/-} mice (Figure 6C, D and Supplementary Information, appendix IV, page 160) providing a molecular rationale for the lower macrophage content in WAT.

MIF-deficiency reduces atherosclerosis associated with IR

Atherosclerosis developed after glucose intolerance/IR and was analyzed in mice maintained on a chow diet for 52 weeks. The aortic plaque load (determined by *en face* Oil-Red O-staining) of *Mif*^{-/-}*Ldlr*^{-/-} mice was lower than in *Ldlr*^{-/-} (Figure 7A). *Mif*^{-/-}*Ldlr*^{-/-} also displayed significantly less atherosclerosis in the aortic valve area of the aortic root (Figure 7B). Analysis of the lesional content of monocytes/macrophages in cross-sections of the aortic root demonstrated a significant reduction in the numbers of these cells in *Ldlr*^{-/-}*Mif*^{-/-} mice (reduced by 5.1-fold $P < 0.05$; Figure 7C and data not shown).

These data are consistent with the observed effects of MIF in WAT, and they support the conclusion that MIF-deficiency impairs the accumulation of monocytes/macrophages in the vascular wall, which is a fundamental, pathologic feature necessary for the development of atherosclerosis.

Discussion

MIF plays pivotal roles in inflammatory diseases and atherogenesis¹⁴ but it has remained unclear whether MIF is causally involved in the development of metabolic disorders associated with obesity and the metabolic syndrome. We show herein that genetic deletion of MIF blocks the development of glucose intolerance, IR and associated atherosclerotic disease. Importantly, MIF-deficiency reduces macrophage infiltration into WAT and lowers both tissue-specific and systemic chronic inflammation without affecting obesity (adiposity) and lipid risk factors. To our knowledge, the present study provides the first experimental evidence for the direct involvement of MIF in the evolution of IR/glucose intolerance and it is consistent with previous reports showing that MIF is a key element in atherogenesis.

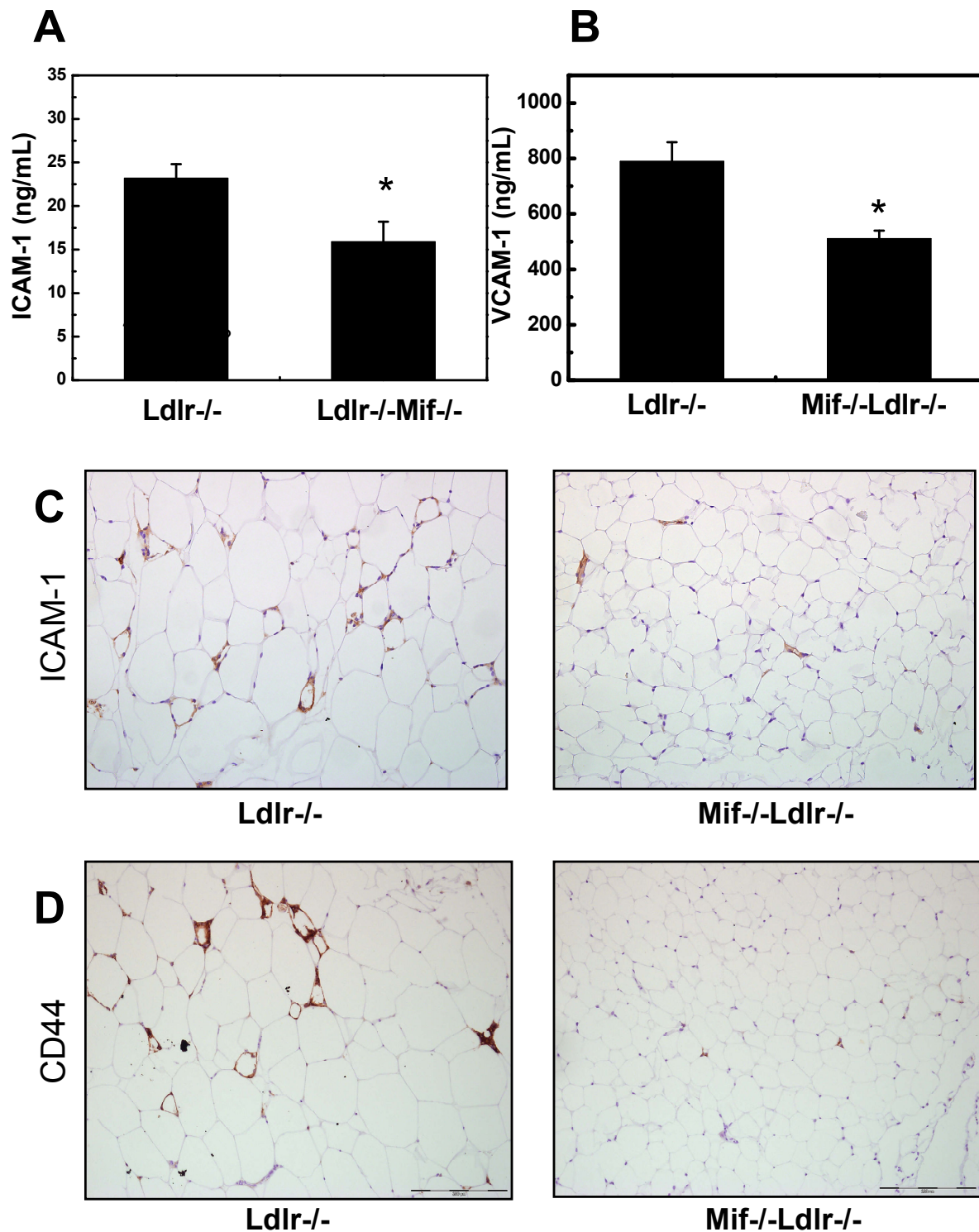


Figure 6: Plasma levels of **A**, ICAM-1 and **B**, VCAM-1 in Ldlr^{-/-} and Mif^{-/-}Ldlr^{-/-} mice. Data shown are absolute values and expressed as means \pm S.D. *Significant difference is indicated *P<0.05. **C**, Representative photomicrographs of epididymal adipose tissue from Ldlr^{-/-} and Mif^{-/-}Ldlr^{-/-} mice stained with an antibody specific for ICAM-1 or **D**, an antibody specific for CD44.

Our observation that MIF-deficiency reduces WAT inflammation and selectively improves the insulin sensitivity of this tissue is consistent with the finding that glucose uptake into WAT is increased in *Mif*^{-/-} mice under conditions of severe inflammation (LPS-induced endotoxemia) with glucose uptake of skeletal muscle and hepatic glucose production being unaffected²⁷.

Chronic low-grade inflammation is considered to be an important risk factor of metabolic and cardiovascular diseases but it is unclear how it can be manipulated without severe consequences to the organism²⁸. Metabolic and immune response pathways are evolutionarily linked and therefore modulation of inflammatory risk factors often affects metabolic risk factors^{8;29}, and vice versa³⁰. For example, deletion of inflammatory cytokines such as IL-1 α , IL-6, IL-18 and TNF α can result in a significant increase in plasma cholesterol²⁹. Also, anti-inflammatory drugs such as acetylsalicylic acid or salicylate can modulate plasma cholesterol levels and considerably affect body weight^{8;31}. Here, we show that MIF-deficiency lowers the inflammatory reactivity without affecting typical metabolic risk factors including plasma triglycerides, free fatty acids, VLDL, LDL, HDL, body weight, adipose mass, voluntary activity and metabolic performance as revealed by the experiments performed in metabolic cages. Compared to *Ldlr*^{-/-} mice, *Mif*^{-/-}*Ldlr*^{-/-} mice display lower levels of systemic (SAA, fibrinogen) and vascular (E-selectin, VCAM-1) inflammation markers, and their WAT contains less macrophages, nucleus-associated c-Jun, ICAM-1 and CD44. One reason for the observed selective reduction in inflammation may be that MIF does not participate in the interface that links metabolic to inflammatory pathways ('metaflammation' pathways²⁸) and that MIF's role within the inflammatory cascade is mainly to amplify and enhance existing inflammatory signals. This amplifier function may explain the large differences in local WAT-specific inflammation observed in this study. Adipose tissue is considered to be an important site for the production of inflammatory mediators²⁸, and it is possible that the lower WAT inflammation observed in the setting of MIF-deficiency is due to both a lower systemic inflammatory response and to a loss of amplifying signals for cytokine (IL-6) and acute phase (CRP, SAA, fibrinogen) responses in the liver. The central role of MIF in amplifying WAT and hepatic inflammation also may explain why MIF correlates well with the systemic inflammatory status of patients in epidemiological studies and why the associations of MIF with impaired glucose tolerance (IGT) and T2D were much stronger than the association between IL-6 or CRP with IGT and T2D³².

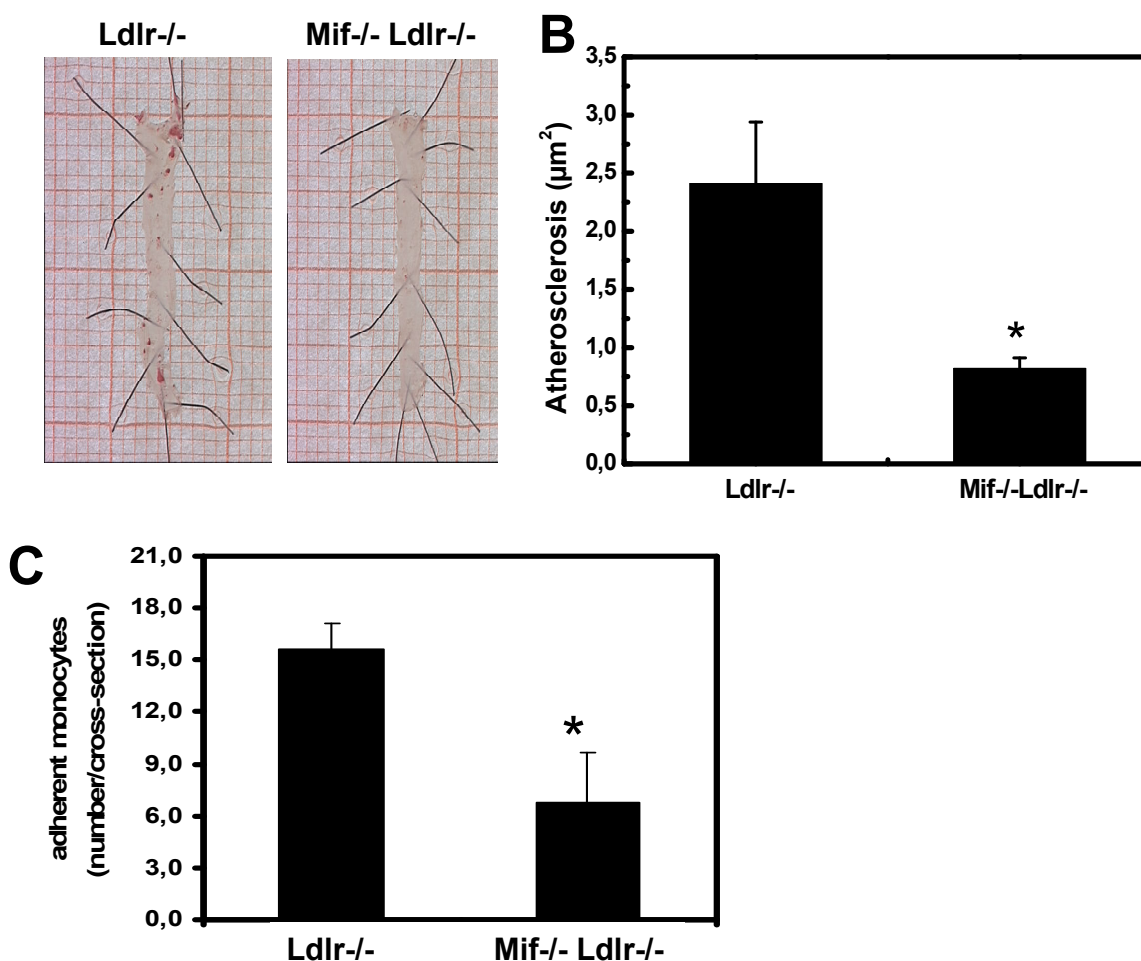


Figure 7: **A**, Representative photomicrographs of *en face* Oil-red O stained aortas from Ldlr-/- and Mif-/-Ldlr-/- mice (35 w of age). **B**, Analysis of atherosclerosis in the aortic valve area of the aortic root (n=12 per group). Significant difference is indicated * P<0.05.

The specific effect of MIF-deficiency on the inflammatory state (but not on lipid/metabolic risk factors) enabled us to study the consequences of a prolonged, selective reduction of inflammation. Our results clearly demonstrate that lowering chronic inflammation *per se* is an effective strategy to block the development of metabolic as well as cardiovascular disease at an early stage. Genetic deletion of MIF thus produces a different phenotype than that resulting from genetic deficiency of CCR2, which encodes a high-affinity ligand of CCL2/MCP-1 that also regulates macrophage infiltration into WAT in the context of IR³³. Genetic deficiency in CCR2 reduces food intake and adiposity thereby attenuating the development of obesity. Our data clearly demonstrate that WAT inflammation and the development of IR can be reduced significantly without affecting the development of obesity. Further research is necessary to understand the selective, obesity-independent effect of MIF on WAT inflammation.

Recent epidemiological data provide support for a role for MIF in the development of IR in humans. Herder and coworkers reported a strong positive association between systemic concentrations of MIF and impaired glucose tolerance and T2D (KORA S4 study; n=1,653)³². High plasma MIF levels also are positively associated with the progression to overt T2D (Finnish Diabetes Prevention Study, n=522)⁶. Additional support for a causal role of MIF in the etiology of T2D comes from a population-based study comparing the effect of single nucleotide polymorphisms of MIF on serum concentrations and the risk of T2D (MONICA/KORA Augsburg Study, n=1134)³⁴. Functional polymorphisms in the MIF promoter have been described that are associated with different inflammatory disorders³⁵. The MIF genotype rs1007888CC was observed to be associated with increased circulating MIF levels and an increased T2D risk³⁴. Interestingly, in male participants of this study, MIF levels were significantly associated with high CRP and IL-6 levels. We found that MIF-expressing mice (independent of the *Ldlr*^{-/-} background) display higher levels of fibrinogen, an IL-6-inducible liver-derived acute phase protein (APP), and SAA, which can be viewed as the murine counterpart of CRP. We also demonstrate that MIF is involved in the constitutive and IL-1-induced expression of SAA. This effect and the finding that MIF stimulates the expression of human CRP *in vivo* as shown in human CRP transgenic mice have not been reported so far.

The role of MIF in the regulation of acute phase genes (e.g. CRP, SAA, and fibrinogen) has not been analyzed systematically. A positive effect of MIF on APP is of great importance because these proteins are not only powerful predictors of disease^{4,36} but also participate in pathophysiological processes leading to the formation of atherosclerotic lesions^{9,37}. Possible sources of pro-atherogenic APP production are WAT and liver. It is well established that very powerful cytokine inducers of hepatic APP expression are IL-1 β and IL-6³⁸, both of which are increasingly expressed during ageing in mouse WAT¹⁰. It is thus possible that the observed differences in APP levels are a consequence of a local effect of MIF in WAT (e.g. on IL-6 release by this tissue). Another explanation may be that MIF controls a transcription factor shared by the various APP. Immunoneutralization of MIF lowers plasma fibrinogen and IL-6 levels and reduces the expression level of C/EBP β a common transcription factor³⁹. C/EBP β is not only a positive regulator of IL-6, fibrinogen, SAA and CRP but also a transcription factor for the adhesion molecules VCAM-1 and ICAM-1⁴⁰, each of which was affected in this study in a MIF-dependent way.

Our data demonstrate that MIF is a central contributor to inflammation in WAT, which likely plays a crucial role in the development of IR³. Xu and coworkers showed that many

inflammation and macrophage-specific genes are significantly upregulated in WAT in mouse models of genetic and high-fat diet-induced obesity leading to IR (*ob/ob*, *db/db*, *agouti* and *tubby* in the C57BL/6J strain)³. The present microarray analyses demonstrate that a similar genetic upregulation occurs in insulin-resistant *Ldlr*^{-/-} mice, indicating that WAT-specific inflammation also develops under the relatively mild experimental conditions of a low-fat chow diet. That the biological processes affected in this study overlapped to a great extent with the pathways identified by Xu et al. (cell division/cell cycle, signal transduction, lipid metabolism/cholesterol metabolism) further substantiates the relevance of these processes for IR in WAT, independent of the model and the dietary conditions applied.

Taken together, our observations support the overall physiological importance of chronic inflammation in the pathogenesis of IR and associated atherosclerosis. Given that the metabolic parameters studied (e.g. triglycerides, free fatty acids, VLDL, LDL, HDL, body weight and adiposity) were unchanged in *Ldlr*^{-/-} and *Mif*^{-/-}*Ldlr*^{-/-} mice, MIF may represent a unique therapeutic target for the specific reduction of WAT inflammation and the ensuing development of cardiovascular and metabolic diseases.

Acknowledgements

We thank Annie Jie and Karin Toet for excellent bioinformatical and analytical help.

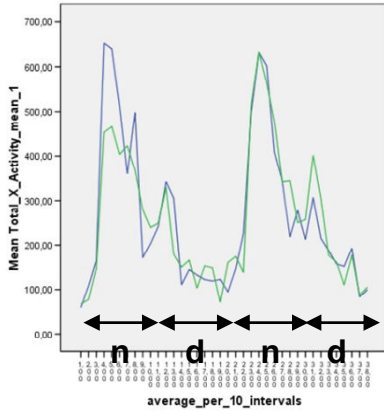
Sources of funding

This study was supported by the Dutch Organization for Scientific Research (NWO Zon-MW; VENI 016. 036.061 to R.K.; VENI 916-36-071 and VIDI 917.76.301 to P.J.V), the Dutch Heart Foundation (grant 2002B102 to L.V.), the TNO research program NISB (to R.K., M.E. and T.K.), the Nutrigenomics Consortium and the Centre for Medical Systems Biology (grant 115) in the framework of the Netherlands Genomics Initiative (to J.d.V.v.d.W. and K.W.v.D), and the US National Institutes of Health (R.B.). The authors acknowledge grant support from the German Research Council (DFG) (SFB 542/TP-A7 and DFG-FOR809/P1 to J.B.; Fi712/2-1 to G.FR.), and from the Cologne Fortune Program of the Medical Faculty of Cologne University (to G.FR.) and from the European Commission (grant COST BM0602 to D.M.O.)

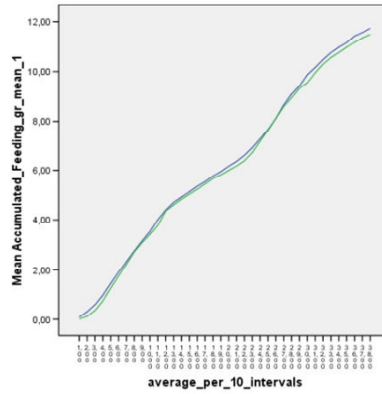
Appendix I

Effect of MIF-deficiency on metabolic performance. Groups of n=8 animals (Ldlr^{-/-}, green; Mif^{-/-}Ldlr^{-/-}, blue) were monitored in computerized metabolic cages.

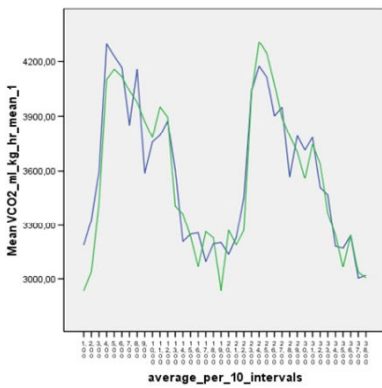
voluntary activity



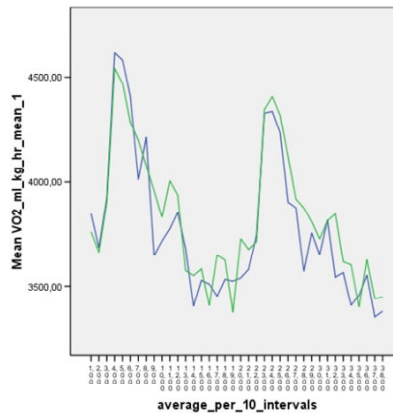
food intake



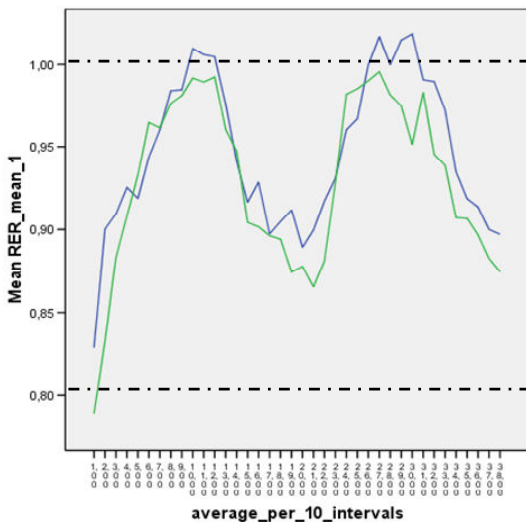
CO₂ production



O₂ consumption



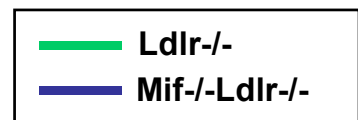
Respiratory exchange ratio



Energy source:

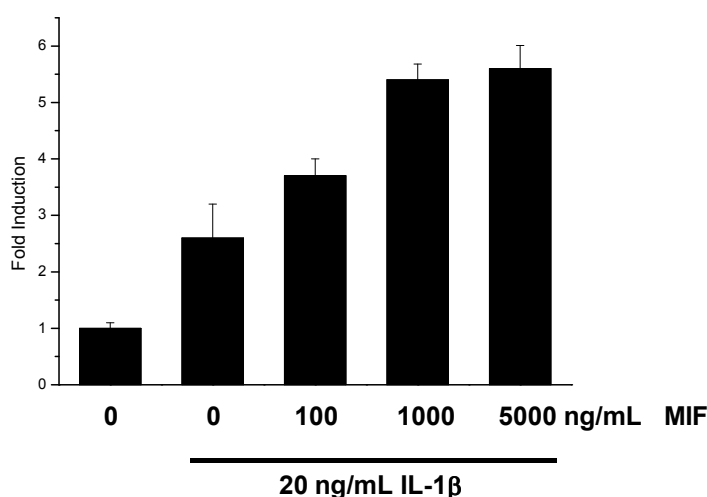
glucose

fat

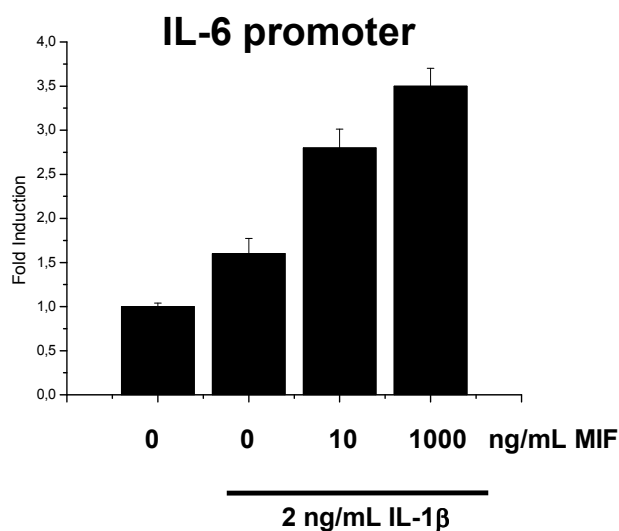


Appendix II

MIF activates the human CRP and human IL-6 promoter. HuH7 hepatoma cells (1.2×10^5) were transiently transfected with 100 ng of a luciferase reporter plasmid carrying a 300-bp fragment of (A) the human CRP promoter or (B) the IL-6 promoter using the FUGENE6 transfection reagent (Roche Diagnostics). Cells were stimulated with cytokines and harvested after 18 h. Reporter gene activity was determined using the dual-luciferase reporter assay system (Promega). A renilla luciferase constructed was co-transfected to correct for differences in transfection efficiency.

A CRP promoter

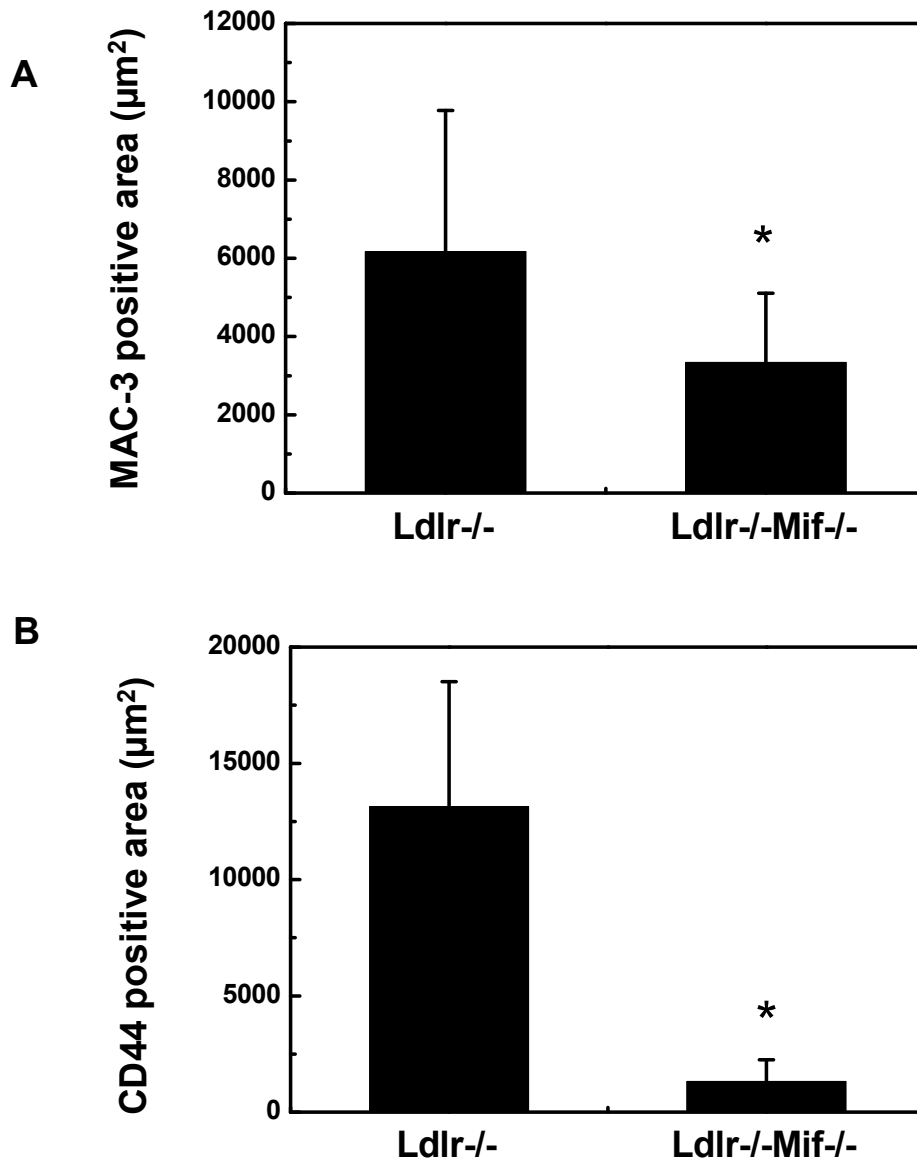
Maximal stimulating effect of MIF alone (1.8-fold induction; not shown)

B IL-6 promoter

Maximal stimulating effect of MIF alone (1.5-fold induction; not shown)

Appendix III

Effect of MIF-deficiency on macrophage area and CD44 expression in WAT. Computer-assisted (QWin software; Leica) quantification of the MAC3-positive area and the CD44-positive area in cross-sections prepared from WAT of Ldlr^{-/-} and Mif^{-/-}Ldlr^{-/-} mice. *P<0.05 indicates significant differences.



Appendix IV

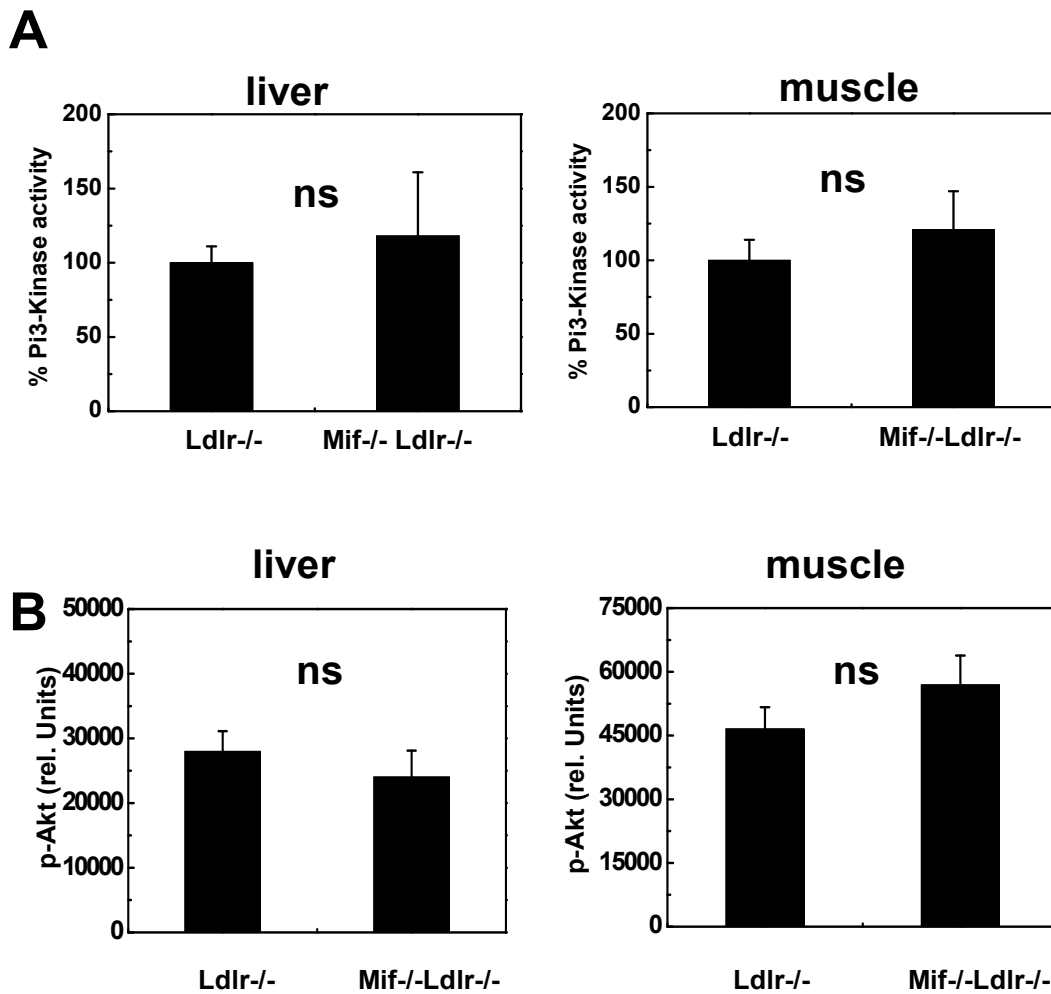
Overview of pathways in epididymal adipose tissue that are affected in *Ldlr*^{-/-} as compared to *Mif*^{-/-}*Ldlr*^{-/-}. Differentially expressed genes were analyzed across pathways using MetaCore™ software and according to standard Gene Ontology (GO) Biological Process nomenclature. Biological categories and functional processes are listed together with their *P*-value.

Processes affected by MIF in epididymal adipose tissue

Biological category	Functional process	<i>P</i>-value
Cell signaling	IGF-R1 signalling	0.04
	leptin signalling via JAK/STAT and MAPK cascades	0.04
	Insulin receptor pathway signalling	0.10
	Signaling through ASK1	0.001
	Signaling pathway mediated by IL-6 and IL-1	0.06
Cell cycle control	Nucleocytoplasmic transport of CDK/cyclins	0.02
	ATM/ATR regulation of G2/M checkpoint	0.04
	Cell cycle regulation by 14-3-3 proteins	0.03
Immune response	Innate immunity responses	0.06
	ERK interactions	0.06
	Integrin-mediated cell adhesion	0.10
	IL-3 activation and signaling	0.06
(Lipid) metabolism	Cholesterol biosynthesis	0.02
	PPAR regulation of lipid metabolism	0.03
	Prostaglandin 1 biosynthesis and metabolism	0.001
	Unsaturated fatty acid biosynthesis	0.04

Appendix V

Effect of MIF-deficiency on PI3-kinase and p-AKT in liver and muscle. PI3-kinase activity and p-AKT levels in liver and muscle. Ldlr^{-/-} and Ldlr^{-/-}Mif^{-/-} mice (n=7 each) were sacrificed precisely 10 min after treatment with 0.5 U insulin per 25 g body weight. Data are means \pm SD. Significant differences are indicated *P<0.05.



Reference List

- (1) Neels JG, Olefsky JM. Inflamed fat: what starts the fire? *J Clin Invest.* 2006;116:33-35.
- (2) Bansilal S, Farkouh ME, Fuster V. Role of insulin resistance and hyperglycemia in the development of atherosclerosis. *Am J Cardiol.* 2007;99:6B-14B.
- (3) Xu H, Barnes GT, Yang Q, Tan G, Yang D, Chou CJ, Sole J, Nichols A, Ross JS, Tartaglia LA, Chen H. Chronic inflammation in fat plays a crucial role in the development of obesity-related insulin resistance. *J Clin Invest.* 2003;112:1821-1830.

- (4) Festa A, D'Agostino R, Jr., Tracy RP, Haffner SM. Elevated levels of acute-phase proteins and plasminogen activator inhibitor-1 predict the development of type 2 diabetes: the insulin resistance atherosclerosis study. *Diabetes*. 2002;51:1131-1137.
- (5) Festa A, D'Agostino R, Jr., Howard G, Mykkanen L, Tracy RP, Haffner SM. Chronic subclinical inflammation as part of the insulin resistance syndrome: the Insulin Resistance Atherosclerosis Study (IRAS). *Circulation*. 2000;102:42-47.
- (6) Herder C, Peltonen M, Koenig W, Kraft I, Muller-Scholze S, Martin S, Lakka T, Ilanne-Parikka P, Eriksson JG, Hamalainen H, Keinanen-Kiukaanniemi S, Valle TT, Uusitupa M, Lindstrom J, Kolb H, Tuomilehto J. Systemic immune mediators and lifestyle changes in the prevention of type 2 diabetes: results from the Finnish Diabetes Prevention Study. *Diabetes*. 2006;55:2340-2346.
- (7) Kaneto H, Nakatani Y, Miyatsuka T, Kawamori D, Matsuoaka TA, Matsuhisa M, Kajimoto Y, Ichijo H, Yamasaki Y, Hori M. Possible novel therapy for diabetes with cell-permeable JNK-inhibitory peptide. *Nat Med*. 2004;10:1128-1132.
- (8) Kleemann R, Verschuren L, van Erk MJ, Nikolsky Y, Cnubben NH, Verheij ER, Smilde AK, Hendriks HF, Zadelaar S, Smith GJ, Kaznatcheev V, Nikolskaya T, Melnikov A, Hurt-Camejo E, van der GJ, van OB, Kooistra T. Atherosclerosis and liver inflammation induced by increased dietary cholesterol intake: a combined transcriptomics and metabolomics analysis. *Genome Biol*. 2007;8:R200.
- (9) O'brien KD, McDonald TO, Kunjathoor V, Eng K, Knopp EA, Lewis K, Lopez R, Kirk EA, Chait A, Wight TN, Debeer FC, Leboeuf RC. Serum amyloid A and lipoprotein retention in murine models of atherosclerosis. *Arterioscler Thromb Vasc Biol*. 2005;25:785-790.
- (10) Wu D, Ren Z, Pae M, Guo W, Cui X, Merrill AH, Meydani SN. Aging up-regulates expression of inflammatory mediators in mouse adipose tissue. *J Immunol*. 2007;179:4829-4839.
- (11) Lue H, Kleemann R, Calandra T, Roger T, Bernhagen J. Macrophage migration inhibitory factor (MIF): mechanisms of action and role in disease. *Microbes Infect*. 2002;4:449-460.
- (12) Zerneck A, Bernhagen J, Weber C. Macrophage migration inhibitory factor in cardiovascular disease. *Circulation*. 2008;117:1594-1602.
- (13) Miller EJ, Li J, Leng L, McDonald C, Atsumi T, Bucala R, Young LH. Macrophage migration inhibitory factor stimulates AMP-activated protein kinase in the ischaemic heart. *Nature*. 2008;451:578-582.
- (14) Morand EF, Leech M, Bernhagen J. MIF: a new cytokine link between rheumatoid arthritis and atherosclerosis. *Nat Rev Drug Discov*. 2006;5:399-410.
- (15) Baugh JA, Bucala R. Macrophage migration inhibitory factor. *Crit Care Med*. 2002;30:S27-S35.
- (16) Bernhagen J, Krohn R, Lue H, Gregory JL, Zerneck A, Koenen RR, Dewor M, Georgiev I, Schober A, Leng L, Kooistra T, Fingerle-Rowson G, Ghezzi P, Kleemann R, McColl SR, Bucala R, Hickey MJ, Weber C. MIF is a noncognate ligand of CXC chemokine receptors in inflammatory and atherogenic cell recruitment. *Nat Med*. 2007;13:587-596.
- (17) Merat S, Casanada F, Sutphin M, Palinski W, Reaven PD. Western-type diets induce insulin resistance and hyperinsulinemia in LDL receptor-deficient mice but do not increase aortic atherosclerosis compared with normoinsulinemic mice in which similar plasma cholesterol levels are achieved by a fructose-rich diet. *Arterioscler Thromb Vasc Biol*. 1999;19:1223-1230.
- (18) Kleemann R, Verschuren L, De Rooij BJ, Lindeman J, De Maat MM, Szalai AJ, Princen HM, Kooistra T. Evidence for anti-inflammatory activity of statins and PPARalpha activators in human C-reactive protein transgenic mice in vivo and in cultured human hepatocytes in vitro. *Blood*. 2004;103:4188-4194.
- (19) Verschuren L, Kleemann R, Offerman EH, Szalai AJ, Emeis SJ, Princen HM, Kooistra T. Effect of low dose atorvastatin versus diet-induced cholesterol lowering on atherosclerotic lesion progression and

- inflammation in apolipoprotein E*3-Leiden transgenic mice. *Arterioscler Thromb Vasc Biol.* 2005;25:161-167.
- (20) Rein D, Schijlen E, Kooistra T, Herbers K, Verschuren L, Hall R, Sonnewald U, Bovy A, Kleemann R. Transgenic flavonoid tomato intake reduces C-reactive protein in human C-reactive protein transgenic mice more than wild-type tomato. *J Nutr.* 2006;136:2331-2337.
- (21) Madsen L, Pedersen LM, Liasset B, Ma T, Petersen RK, van den BS, Pan J, Muller-Decker K, Dulsner ED, Kleemann R, Kooistra T, Dorskeland SO, Kristiansen K. cAMP-dependent signaling regulates the adipogenic effect of n-6 polyunsaturated fatty acids. *J Biol Chem.* 2008;283:7196-7205.
- (22) Voshol PJ, Jong MC, Dahlmans VE, Kratky D, Levak-Frank S, Zechner R, Romijn JA, Havekes LM. In muscle-specific lipoprotein lipase-overexpressing mice, muscle triglyceride content is increased without inhibition of insulin-stimulated whole-body and muscle-specific glucose uptake. *Diabetes.* 2001;50:2585-2590.
- (23) Kolter T, Uphues I, Eckel J. Molecular analysis of insulin resistance in isolated ventricular cardiomyocytes of obese Zucker rats. *Am J Physiol.* 1997;273:E59-E67.
- (24) Kooistra T, Verschuren L, de Vries-van der Weij, Koenig W, Toet K, Princen HM, Kleemann R. Fenofibrate reduces atherogenesis in ApoE*3Leiden mice: evidence for multiple antiatherogenic effects besides lowering plasma cholesterol. *Arterioscler Thromb Vasc Biol.* 2006;26:2322-2330.
- (25) Kleemann R, Kapurniotu A, Frank RW, Gessner A, Mischke R, Flieger O, Juttner S, Brunner H, Bernhagen J. Disulfide analysis reveals a role for macrophage migration inhibitory factor (MIF) as thiol-protein oxidoreductase. *J Mol Biol.* 1998;280:85-102.
- (26) Kleemann R, Rorsman H, Rosengren E, Mischke R, Mai NT, Bernhagen J. Dissection of the enzymatic and immunologic functions of macrophage migration inhibitory factor. Full immunologic activity of N-terminally truncated mutants. *Eur J Biochem.* 2000;267:7183-7193.
- (27) Atsumi T, Cho YR, Leng L, McDonald C, Yu T, Danton C, Hong EG, Mitchell RA, Metz C, Niwa H, Takeuchi J, Onodera S, Umino T, Yoshioka N, Koike T, Kim JK, Bucala R. The proinflammatory cytokine macrophage migration inhibitory factor regulates glucose metabolism during systemic inflammation. *J Immunol.* 2007;179:5399-5406.
- (28) Hotamisligil GS. Inflammation and metabolic disorders. *Nature.* 2006;444:860-867.
- (29) Kleemann R, Zadelaar S, Kooistra T. Cytokines and atherosclerosis: a comprehensive review of studies in mice. *Cardiovasc Res.* 2008.
- (30) Zadelaar S, Kleemann R, Verschuren L, de Vries-van der Weij, van der HJ, Princen HM, Kooistra T. Mouse models for atherosclerosis and pharmaceutical modifiers. *Arterioscler Thromb Vasc Biol.* 2007;27:1706-1721.
- (31) Patel DG, Skau KA. Effects of chronic sodium salicylate feeding on the impaired glucagon and epinephrine responses to insulin-induced hypoglycaemia in streptozotocin diabetic rats. *Diabetologia.* 1989;32:61-66.
- (32) Herder C, Kolb H, Koenig W, Haastert B, Muller-Scholze S, Rathmann W, Holle R, Thorand B, Wichmann HE. Association of systemic concentrations of macrophage migration inhibitory factor with impaired glucose tolerance and type 2 diabetes: results from the Cooperative Health Research in the Region of Augsburg, Survey 4 (KORA S4). *Diabetes Care.* 2006;29:368-371.
- (33) Weisberg SP, Hunter D, Huber R, Lemieux J, Slaymaker S, Vaddi K, Charo I, Leibel RL, Ferrante AW, Jr. CCR2 modulates inflammatory and metabolic effects of high-fat feeding. *J Clin Invest.* 2006;116:115-124.
- (34) Herder C, Klopp N, Baumert J, Muller M, Khuseyinova N, Meisinger C, Martin S, Illig T, Koenig W, Thorand B. Effect of macrophage migration inhibitory factor (MIF) gene variants and MIF serum

concentrations on the risk of type 2 diabetes: results from the MONICA/KORA Augsburg Case-Cohort Study, 1984-2002. *Diabetologia*. 2008;51:276-284.

- (35) Meyer-Siegler KL, Vera PL, Iczkowski KA, Bifulco C, Lee A, Gregersen PK, Leng L, Bucala R. Macrophage migration inhibitory factor (MIF) gene polymorphisms are associated with increased prostate cancer incidence. *Genes Immun*. 2007;8:646-652.
- (36) Ridker PM, Stampfer MJ, Rifai N. Novel risk factors for systemic atherosclerosis: a comparison of C-reactive protein, fibrinogen, homocysteine, lipoprotein(a), and standard cholesterol screening as predictors of peripheral arterial disease. *JAMA*. 2001;285:2481-2485.
- (37) Pasceri V, Willerson JT, Yeh ET. Direct proinflammatory effect of C-reactive protein on human endothelial cells. *Circulation*. 2000;102:2165-2168.
- (38) Kleemann R, Gervois PP, Verschuren L, Staels B, Princen HM, Kooistra T. Fibrates down-regulate IL-1-stimulated C-reactive protein gene expression in hepatocytes by reducing nuclear p50-NFkappa B-C/EBP-beta complex formation. *Blood*. 2003;101:545-551.
- (39) Burger-Kentischer A, Gobel H, Kleemann R, Zerneck A, Bucala R, Leng L, Finkelmeier D, Geiger G, Schaefer HE, Schober A, Weber C, Brunner H, Rutten H, Ihling C, Bernhagen J. Reduction of the aortic inflammatory response in spontaneous atherosclerosis by blockade of macrophage migration inhibitory factor (MIF). *Atherosclerosis*. 2006;184:28-38.
- (40) Carter AM. Inflammation, thrombosis and acute coronary syndromes. *Diab Vasc Dis Res*. 2005;2:113-121.